Int. J. Rock Mech. Min. Sci. & Geomech. Abstr. Vol. 13, pp. 53–59. Pergamon Press 1976. Printed in Great Britain

Microcrack Nucleation in Marble

WILLIAM A. OLSSON*
SYD S. PENG†

In this study it has been found that in marble the inhomogeneous nature of plastic flow on the scale of the grain size can result in the nucleation of microcracks. Specimens of Tennessee marble were deformed in compression at confining pressures of 0–46 MN/m² and at a strain rate of 10^{-5}/sec. Four types of microcrack nucleation mechanisms have been identified. Types I and II operate at the intersections of glide lamellae with grain boundaries. The crack forms at a high angle to the lamellae in the type I case, and parallel to the lamellae in the type II case. The microcrack resulting from the operation of a type III mechanism forms at the intersections of lamellae; that from a type IV is caused by a wedging action of a combination of weak and strong grains. Mechanisms I, III and IV lead to microcracks subparallel to the direction of maximum compression. Mechanism II produces a crack lying in a plane of high shear stress. Faults are composed of en echelon arrays of subaxial cracks connected by packets of inclined twin lamellae.

INTRODUCTION

In rock fracture analyses, three sequential events are most often discussed: initiation, propagation, and coalescence of cracks leading to the ultimate fracture. 'Initiation' of cracks appears to refer to the beginning of the extension of a preexisting Griffith crack [2, 4, 6, 14]. Although numerous studies [for example 3, 20, 24, 29] have revealed that rocks possess abundant microcracks that may propagate under favorable conditions, there is evidence that cracks can be formed in a previously 'continuous' material [25, 30]. The process of forming new cracks, referred to in the metallurgical literature [26] as crack nucleation, has been only briefly described for rock [16]. It is clear that a rational rock fracture criterion based on microcracking should treat crack nucleation as the first sequential event, followed by initiation, propagation and coalescence of cracks. The main objective of the investigation was to determine whether crack nucleation mechanisms similar to those that are discussed in the metallurgical literature [e.g. 26] may operate in some types of rock.

In this paper several mechanisms for the nucleation of microcracks in rock are described in detail. These mechanisms, which have been observed to operate in marble, require plastic deformation in the form of glide lamella formation prior to microcracking.

As is well known, measured fracture strengths of solids are generally several orders of magnitude less than the theoretical cohesive strength. This is primarily because of local stress concentrations that cause crack nucleation and spreading. Such local stress concentrations are usually the result of abrupt changes in some mechanical property, such as the plastic yield stress or elastic modulus, which can produce displacement incompatibilities.

Numerous stress concentrations occur in marble where glide lamellae are blocked by obstacles to glide. Usually this obstacle is a grain boundary, but occasionally it is another lamella. The lamellae which formed in the Tennessee marble in this study were most probably the result of crystallographic twin gliding [28]. When a lamella forms, the shear stress is relaxed within the lamella and is concentrated at the edges [30]. One of two things may happen to relieve this concentrated stress [26]: if the shear stress ahead of the lamella tip, resolved onto a potential glide plane, exceeds a critical value, then glide can be initiated in the vicinity of the lamella tip; if on the other hand, the resolved shear stress is not sufficiently large to initiate slip, then the concentrated normal (tensile) stress may nucleate a crack. The first possibility is illustrated in Fig. 1. In this instance three lamellae have impinged upon a grain boundary (a possible strong obstacle to glide) and caused shear stress concentrations sufficiently large to initiate glide in the next grain. This paper is concerned mainly with the second possibility—that is, when crystallographic misorientation was apparently such that the shear stress resolved onto a potential glide plane was not large enough to initiate glide, but the local tensile stress was strong enough to nucleate a microcrack.

*Twin Cities Mining Research Center, Bureau of Mines, U.S. Department of the Interior, P.O. Box 1660, Twin Cities, Minnesota 55111, U.S.A.

† School of Mines, West Virginia University, Morgantown, West Virginia 26505, U.S.A.

Fig. 1. Twin lamellae causing twin initiation (arrows) across a grain boundary. Maximum compression is vertical. Scale bar is 0·1 mm.

Material and techniques

To avoid some of the complexities introduced by the presence of several minerals with widely differing mechanical properties, the monomineralic Tennessee marble was chosen for the study. This rock is a pinkish gray orthomarble with grain size ranging from 0·01 to 10 mm. It consists of 98·0% calcite and 2·0% clay minerals [27]. About 60% of the grains in the starting material are moderately to highly twinned. No cracks or open grain boundaries were observed at magnifications up to 450 in polished surfaces of the specimens used.

The specimens were rectangular prisms 2·54 cm long with 1·27 cm square cross sections. Before testing, three of the long sides of each specimen were polished so that the experimentally induced deformation features could be clearly distinguished from the previously existing ones when examined under a microscope using vertically incident light. Using vertically incident light allows one to distinguish between the preexisting lamellae and those produced during an experiment.

The specimens were air-dried and jacketed in thin-walled, pliable rubber tubing, and then tested in a closed-loop servocontrolled hydraulic testing machine described elsewhere [19]. Tests were run at room temperature, confining pressures of 0, 23, and 46 MN/m^2, and a strain rate of 10^{-5}/sec. One specimen at 0 MN/m^2 and one at 23 MN/m^2 confining pressure were loaded incrementally along the load–deformation curve. That is, the specimens were first loaded to some arbitrary level, and then unloaded, removed from the testing machine, examined under the microscope, and photographed. This procedure was then repeated an additional five times on the specimen tested at 0 MN/m^2, and an additional four times on the specimen tested at 23 MN/m^2. To determine the extent of grain boundary sliding, one side of the specimen tested incrementally at 23 MN/m^2 confining pressure was coated with fine parallel gold-palladium foil lines, spaced about 80 per cm. These lines were oriented perpendicularly to the maximum compression. Offsets in these lines after testing would indicate sliding on inclined surfaces.

The remainder of the specimens were loaded only once at a given confining pressure, and then examined and photographed. At each of the two higher confining pressures, 23 MN/m^2 and 46 MN/m^2, one specimen was loaded to the vicinity of the yield point, one to the ultimate strength, and one to about 3% reduction in length.

OBSERVATIONS

Microcrack nucleation mechanisms

The microcrack nucleation mechanisms observed to operate in Tennessee marble are idealized in Fig. 2 and labeled I–IV. The type I mechanism was first proposed by Zener [30] and later studied theoretically by Stroh [25]; a typical example from the Tennessee marble is illustrated in Fig. 3A. In this instance, a packet of twin lamellae which intersected a grain boundary caused the tensile stress concentration which nucleated the crack. In general, a crack may form in the grain containing the lamella, in the adjoining grain, or along the grain boundary depending on the relationships between the calculated optimal microcrack orientation [25] and the directions of planes of weakness—cleavage or grain boundaries. All three microcrack orientations have been observed in deformed specimens of Tennessee marble.

The type II mechanism (Figs. 2 and 3B) was first suggested by Bullough in analogy with fractures in bub-

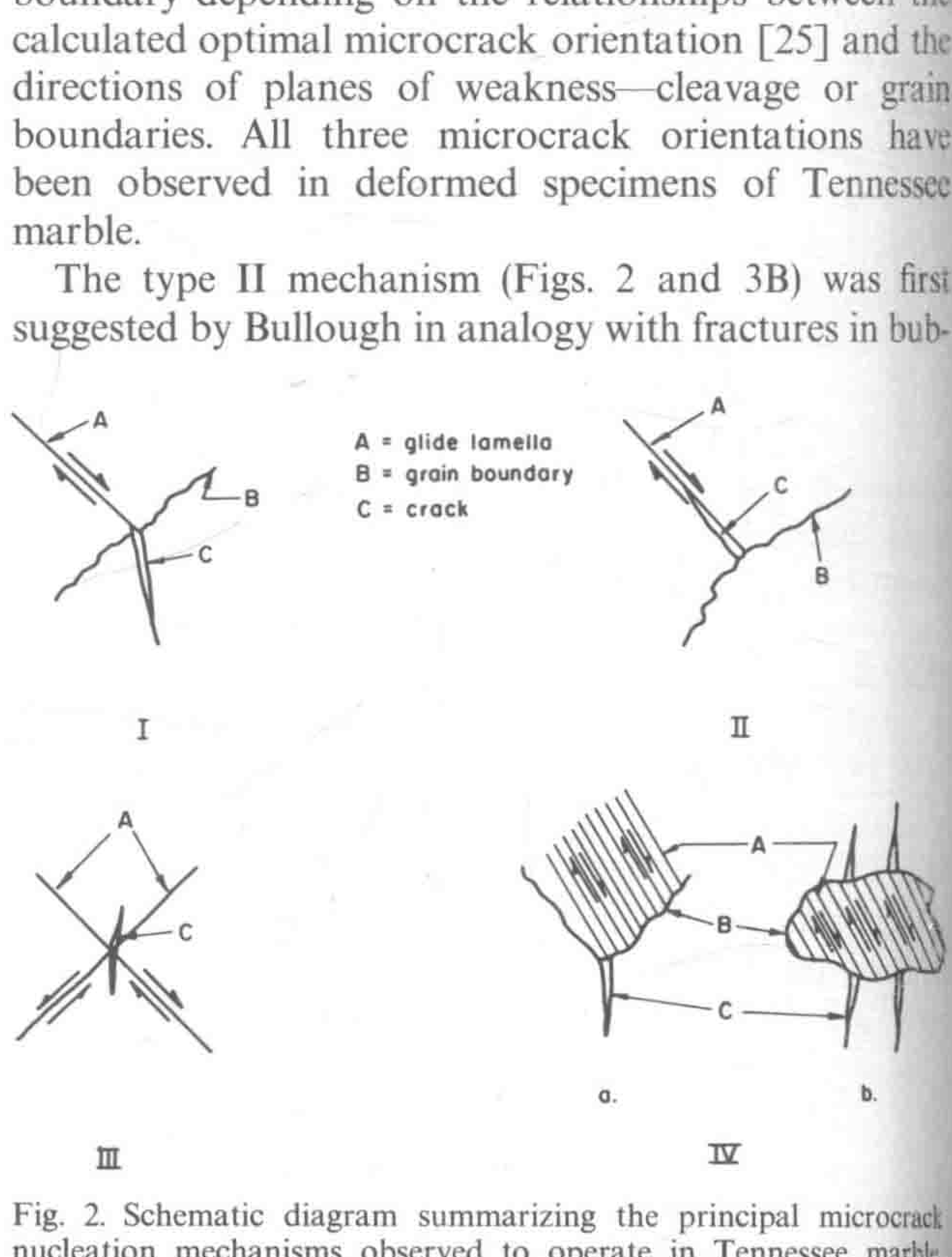

Fig. 2. Schematic diagram summarizing the principal microcrack nucleation mechanisms observed to operate in Tennessee marble. Maximum compression is vertical. The single-sided arrows indicate displacement on lamellae.

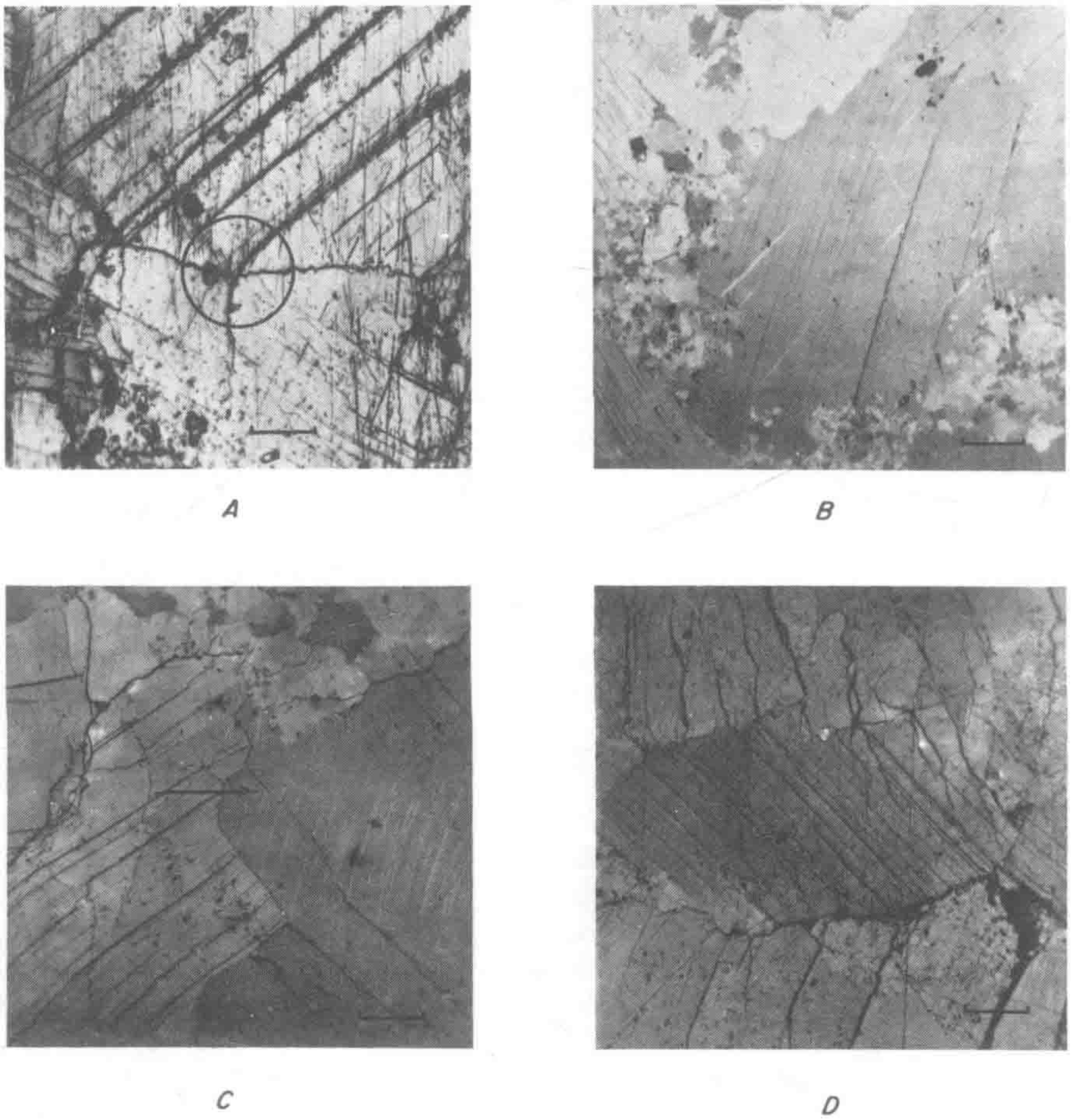

Fig. 3. Photomicrographs of the four types of microcrack nucleation mechanisms found in Tennessee marble. Maximum compression is vertical, and scale bars are 0·1 mm. (A) Type I—Circle encompasses the vertical crack, horizontal grain boundary and the inclined packet of lamellae. (B) Type II—The north-northeast trending dark line is the cracked lamella. (C) Type III—The light toned lines are natural lamellae and the dark line trending northwest is an experimentally produced lamella. The arrow indicates a typical crack nuclei. (D) Type IV—The elliptical grain is highly twinned and the cracks are vertical.

ble rafts (cited in Deruyttere & Greenough [9] and elaborated upon by Gilman [13]). Although the basic geometry of a glide lamella blocked by an obstacle is identical to the type I mechanism, in this instance the crack forms along the lamella. This type of microcrack was infrequently observed in the marble. Because there is a component of compressive stress normal to the glide plane in compression tests, the crack may not actually form until removal of the applied stresses. Hence, this mechanism probably does not contribute to the microcracking during the actual deformation of the marble.

The third mechanism (Figs. 2 and 3C) is the only one observed in Tennessee marble to create microcracks that do not require the presence of a grain boundary; the obstacle to glide is provided by other lamellae rather than a grain boundary. Thus this mechanism could nucleate cracks in single crystals as well as polycrystals. The light-toned lines in the large grain to the right in Fig. 3C are natural lamellae, whereas the dark line trending northwest–southeast is an experimentally produced lamella. Note that a small crack has formed at each intersection of the newly formed lamella with a previously existing lamella. This particular type of microcrack was not often observed in the present study.

The type IV mechanism is comprised of a plastically yielding grain surrounded by non-yielding grains (Figs. 2 and 3D). This has been referred to as the soft inclusion mechanism, and in an earlier study [18] was observed to cause many microcracks in a limestone. In a monomineralic material such as marble, the difference in strength between the inclusion and the surround can be caused by distinct dissimilarities in grain size [5, 17] or by differences in crystallographic orientation [28], among other things. The type IV mechanism also occurs in areas where a weaker grain adjoins a stronger grain and wedges a grain boundary open by its flattening or asymmetric response to the applied compression. Figure 4 shows three photomicrographs taken of the same area on a specimen loaded to positions on the load–deformation curve as indicated. The surface of this particular specimen had been coated prior to deformation with a gold–palladium foil for observation in the scanning electron microscope. The foil broke off the deformed areas of the underlying rock, causing these areas to appear dark. In Fig. 4A several twin lamellae have formed in grain 2 and the boundary

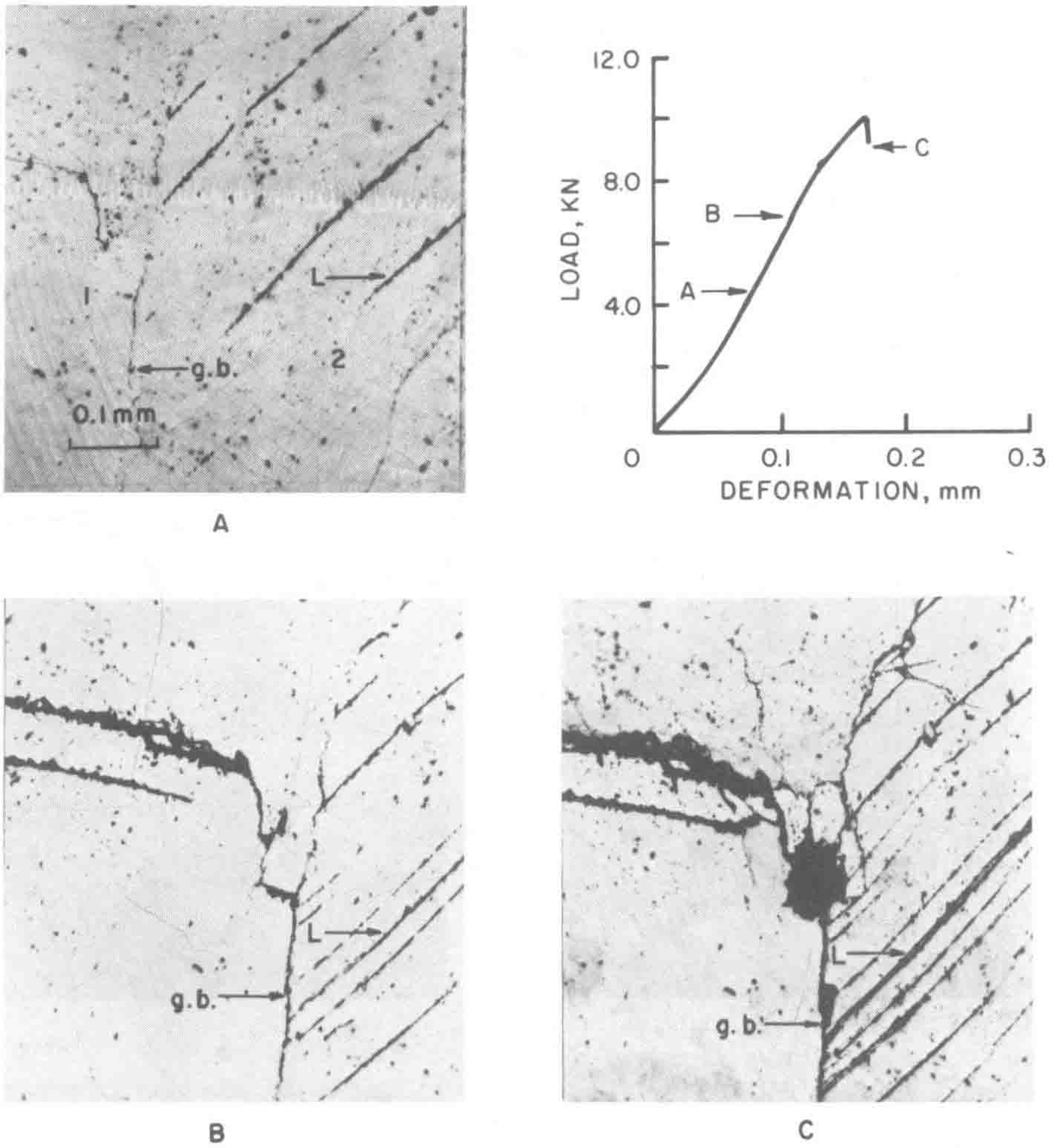

Fig. 4. Sequential photomicrographs showing development of a type IV microcrack nucleation mechanism. Photomicrographs are keyed to the load–deformation plot. Observe the propagation of a lamella (L) and progressive cracking of the grain boundary (g.b.). Maximum compression is vertical. Grains designated 1 and 2 are referred to in the text. Tested in unconfined compression.

separating grain 1 from grain 2 is just barely visible; it is not yet cracked open. In Fig. 4B there is much more extensive lamella development, and the plastic deformation of grain 2, occurring in juxtaposition to the non-yielding grain 1, resulted in the cracking open of the boundary. An interesting observation is that the lamellae appear to spread with increasing deformation rather than to form suddenly at some critical stress level. This may be seen by comparing the lamella marked by L in Figs. 4A, B.

Grain boundary sliding has been suggested as a mechanism for creating microcracks at grain boundary triple junctions [7], and at asperities on the boundary itself [14]. To determine the extent of grain boundary sliding in Tennessee marble, one specimen was coated with fine parallel reference lines spaced about 80 per cm oriented perpendicularly to the maximum compression, and then deformed at 23 MN/m^2 confining pressure (Fig. 5). Any grain boundary sliding should have produced detectable offsets in these lines at their intersections with the grain boundaries. Although the technique was sufficiently sensitive to show small deformations resulting from the formation of twin lamella packets, no grain boundary sliding could be detected until well after the ultimate strength, at which point (Fig. 5C) sharp offsets in the reference lines become apparent. This observation is consistent with the recent report of Bombolakis [3] who found little sliding on inclined surfaces in a granite in the early stages of deformation. Presumably, higher confining pressure would suppress grain boundary sliding even more.

Microcrack nucleation mechanisms I and IV were the most frequently observed ones in Tennessee marble. Examination of specimens compressed to different stress levels shows that deformation lamellae begin to form at applied stresses as low as about 30% of the ultimate strength. Type I cracks begin to form at about 50% of the ultimate strength. Finally, at about 90% of the ultimate strength the type IV mechanisms become operative. Confining pressure tends to increase the stress levels at which twinning and, hence, microcrack nucleation start. This conclusion is consistent with that of other investigators in that the stress levels at the onset of dilatancy [7, 12] and of acoustic emissions [22, 27] are raised by increased confining pressure. In the unconfined compression tests, the crack nuclei generated by mechanisms I and IV sometimes propa-

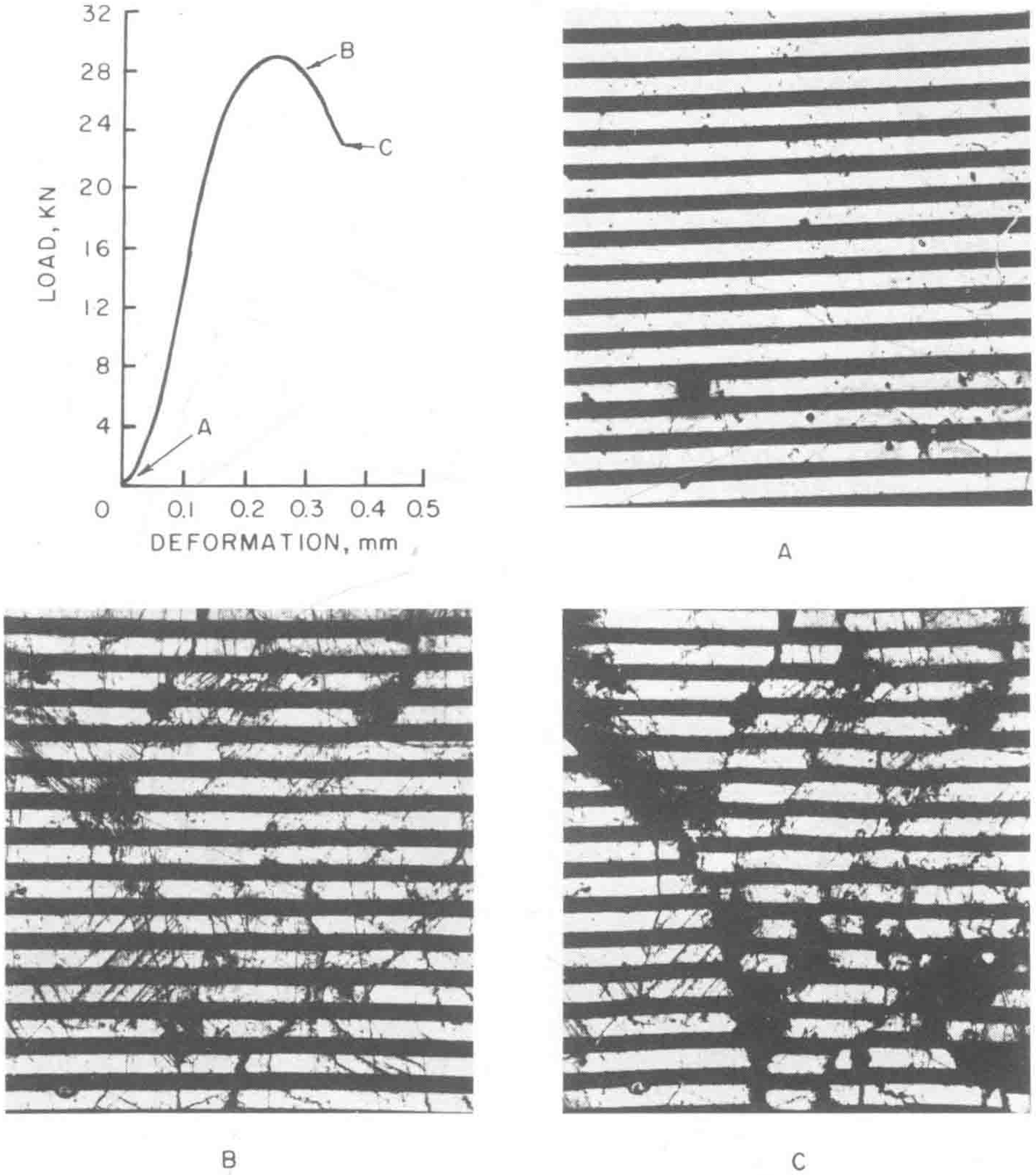

Fig. 5. Sliding on grain boundaries and cracks as revealed by reference bands of gold-palladium foil. Bands are 0·127 mm wide. Photomicrographs are keyed to the load–deformation plot. Maximum compression is vertical and the confining pressure is 23 MN/m^2.

gated axially for distances of several grain diameters or more, leading eventually to macroscopic extension fractures. At 23 MN/m^2 and 46 MN/m^2 confining pressure, however, the crack nuclei seldom propagated more than some fraction of a grain diameter.

Faults

When tested in unconfined compression, the Tennessee marble fails by extension fracturing. However, at the two higher confining pressures, 23 MN/m^2 and 46 MN/m^2, faults are developed at stresses near the ultimate strength. In a specimen tested at a confining pressure of 23 MN/m^2 a type I crack nucleation mechanism was observed at low strain and again at several higher strains as shown in Fig. 6. At load A (Fig. 6A) the type I mechanism was fully developed. At B the zone of deformation, in the form of inclined lamellae and subaxial cracks, had spread out from this nucleus in both directions to form a fault zone. In this instance, the crack nucleation mechanism was also instrumental in initiating the fault. Quite generally, faults in the Tennessee marble are complex tabular zones consisting of both plastic and brittle features. The idealized fault is a sequence of inclined twin lamellae alternating with subaxial cracks. No specimen was compressed to high enough strain to cause the faults to lose cohesion. These faults are geometrically similar to those observed in a sandstone by Dunn *et al.* [11]. A comparison of the present description of a fault in marble to that of a fault in sandstone [11] shows that there are two fundamental differences between faults in these two rocks. First, the inclined elements contributing to the faults in marble are lamellae or packets of lamellae, whereas the inclined elements in sandstone are grain boundaries. Second, Dunn *et al.* [11] concluded that the formation of the subaxial cracks allowed the grain boundaries to slide; this is in contrast to the mechanism in marble where formation of the inclined lamellae causes the subaxial cracks.

DISCUSSION

Stroh [25] developed a criterion for the type I crack nucleation mechanism. According to his model, a crack is nucleated by the stress concentration at the tip of a dislocation pile-up. Although examination of the surfaces of deformed specimens etched in formic acid according to the technique of Keith & Gilman [15]

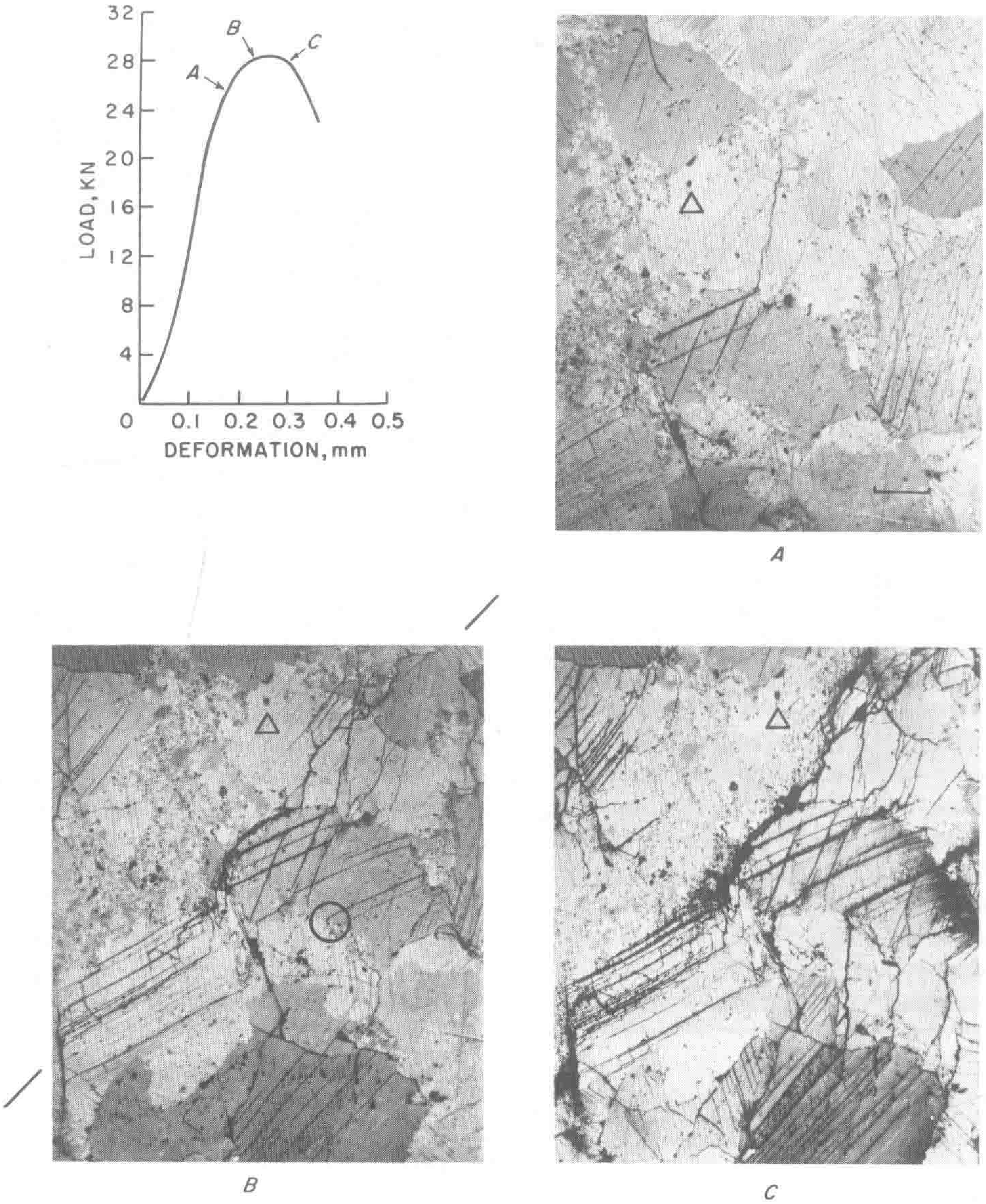

Fig. 6. Progressive formation of a fault from a type I microcrack nucleation mechanism. Maximum compression is vertical, confining pressure was 23 MN/m^2, and the scale bar is 0·1 mm. The △ marks the same point on the three photomicrographs which are keyed to the load–deformation plot. The trend of the fault zone is indicated in (B). (A) Type I nucleation mechanism consisting of an inclined lamella and a vertical crack. (B) The deformation has spread out in an inclined zone from the type I mechanism. Several new type I mechanisms have formed and a typical one is circled. (C) The final fault consisting of inclined lamellae, axial cracks, and parted grain boundaries.

revealed a few dislocation pile-ups at grain boundaries, the lamellae which give rise to microcracks in Tennessee marble invariably appeared to be twin lamellae. Stroh's [25] model is probably applicable in this case because the stress field at the tip of a twin lamella can be approximated by dislocation pile-ups.

Type IV crack nucleation occurred when a softer (weaker) grain was in juxtaposition to harder (stronger) ones. The cracks usually nucleated at the boundary and within the hard grains, and then grew parallel to the direction of applied load. An analysis of the stress concentrations owing to inclusions under various conditions [10] reveals that for an inclusion of certain simple geometry, the magnitude of tensile tangential stresses at the boundary of the inclusion is inversely proportional to the confining pressure and the Young's modulus ratio of inclusion to surround. A crack nucleates in the surround as soon as the local concentrated stresses exceed the tensile strength; the stress level for nucleation in this instance is dependent on confining pressure.

The present results have some bearing on the mechanisms of creep in rock. Scholz [23] considered the phenomenon of stress corrosion cracking and derived a creep law for brittle rock; in effect, time-dependent microcracking causes creep. Alternatively, Savage & Mohanty [21] argued that the time-dependent cracking in brittle rock is due to creep, and that microfractures relieve stress concentrations caused by plastic flow—that is, creep causes microcracking. The observations presented here support this latter view with regard to marble because the cracks were created in response to plastic glide. However, it is not suggested that the mechanisms that operate in marble are relevant to the brittle silicate rocks which Scholz [23] considered.

Another aspect of rock deformation to which the present results apply is that of dilatancy. Recently, Bell & Nur [1] proposed a model of dilatancy based on the results of Stroh [25]. This model allowed them to calculate crack width and thus dilatant strain as functions of shear stress. In their model, the lamella of the type I mechanism described here is treated formally as a dislocation pile-up. When the shear stress on the plane of the pile-up reaches some critical value, dislocations at the tip of the pile-up coalesce to nucleate a microcrack.

Thus the observations presented here lead to a better understanding of the initial stages of deformation of marble and may have several potentially useful applications in rock mechanics problems.

CONCLUSIONS

Four types of microcrack nucleation mechanisms ave been observed to operate in marble tested in comression at very low confining pressures. Types I and I operated at the intersections of glide lamellae with rain boundaries. The crack formed at a high angle o the glide lamella in the type I mechanism, and parall to the lamella in the type II. The microcrack resultng from the operation of a type III mechanism formed t the intersection of two or more glide lamellae. The ype IV mechanism caused a crack by the wedging ction of a combination of weak and strong grains. Mechanisms I, III, and IV led to microcracks subparall to the direction of maximum compression; mechanism II produced a crack lying in a plane of igh shear stress. Mechanisms I and IV were most freuently observed.

Grain boundary sliding in one specimen tested at 3 MN/m^2 confining pressure was found to be insignificant until well after the ultimate strength. Faults were mposed of sequences of en echelon arrays of subaxial acks connected by inclined twin lamellae, or packets lamellae.

knowledgements—This work was done while the senior author d a National Research Council–Bureau of Mines post-doctoral earch associateship.

ceived 20 *May* 1975.

REFERENCES

Bell L. & Nur A. A micromechanical model for dilatancy. *EOS Trans. Am. Geophys. Union*, Abstract **55**, 432 (1974).
2. Bieniawski Z. T. Mechanism of brittle fracture of rock. *Int. J. Rock Mech. Min. Sci.* **4**, 395–406 (1967).
3. Bombolakis E. G. Study of the brittle fracture process under uniaxial compression. *Tectonophysics* **18**, 231–248 (1973).
4. Brace W. F. An extension of the Griffith theory of fracture to rocks. *J. Geophys. Res.* **65**, 3477–3480 (1960).
5. Brace W. F. Dependence of fracture strength of rocks on grain size. *Fourth Symposium on Rock Mechanics, Bull.* Mineral Industries Exp. Stat., Penn. State Univ., **76**, 99–103 (1961).
6. Brace W. F. & Bombolakis E. G. A note on brittle crack growth in compression. *J. Geophys. Res.* **68**, 3709–3713 (1963).
7. Brace W. F., Paulding B. W., Jr. & Scholz C. Dilatancy in the fracture of crystalline rocks. *J. Geophys. Res.* **71**, 3939–3953 (1966).
8. Chang H. C. & Grant N. J. Mechanism of intercrystalline fracture. *Trans. Am. Inst. Min. Engrs* **206**, 544–551 (1956).
9. Deruyttere A. & Greenough G. B. The criterion for the cleavage fracture of zinc single crystals. *J. Inst. Metals* **84**, 337 (1956).
10. Donnell L. H. Stress concentrations due to elliptical discontinuities in plates under edge forces. T. Von Karman Anniversary Volume, California Inst. Tech., Pasadena, CA, 239–309 (1941).
11. Dunn D. E., LaFountain L. J. & Jackson R. E. Porosity dependence and mechanism of brittle fracture in sandstone. *J. Geophys. Res.* **78**, 2403–2417 (1973).
12. Edmond J. M. & Paterson M. S. Volume changes during the deformation of rocks at high pressures. *Int. J. Rock Mech. Min. Sci.* **9**, 161–182 (1972).
13. Gilman J. J. Fracture of zinc-monocrystals and bicrystals. *Trans. Am. Inst. Min Engrs* **212**, 783–791 (1958).
14. Hoek E. & Bieniawski Z. T. Brittle fracture propagation in rock under compression. *Int. J. Fract. Mech.* **1**, 137–155 (1965).
15. Keith R. E. & Gilman J. J. Dislocation etch pits and plastic deformation in calcite. *Acta Metall.* **8**, 1–10 (1960).
16. Olsson W. A. Microcrack nucleation mechanisms in marble (abstract). *EOS Trans. Am. Geophys. Union* **55**, 421 (1974).
17. Olsson W. A. Grain size dependence of yield stress in marble. *J. Geophys. Res.* **79**, 4859–4862 (1974).
18. Olsson W. A. Microfracturing and faulting in a limestone. *Tectonophysics* **24**, 277–285 (1974).
19. Peng S. S. & Podnieks E. R. Relaxation and the behavior of failed rock. *Int. J. Rock Mech. Min. Sci.* **9**, 699–712 (1972).
20. Peng S. S. & Johnson A. M. Crack growth and fracture of Chelmsford Granite. *Int. J. Rock Mech. Min. Sci.* **9**, 37–86 (1972).
21. Savage J. C. & Mohanty B. B. Does creep cause fracture in brittle rock? *J. Geophys. Res.* **74**, 4329–4332 (1969).
22. Scholz C. H. Microfracturing and the inelastic deformation of rock in compression. *J. Geophys. Res.* **73**, 1417–1432 (1968).
23. Scholz C. H. Mechanism of creep in brittle rock. *J. Geophys. Res.* **73**, 3295–3302 (1968).
24. Sprunt E. & Brace W. F. Direct observation of microcavities in crystalline rocks. *Int. J. Rock Mech. Min. Sci. & Geomech. Abstr.* **12**, 139–150 (1974).
25. Stroh A. N. The formation of cracks as a result of plastic flow. *Proc. R. Soc.* A**223**, 404–414 (1954).
26. Tetelman A. S. & McEvily A. J., Jr. *Fracture of Structural Materials*, Wiley, New York (1967).
27. Thill R. E. Acoustic methods for monitoring failure in rock. *Proc. Fourteenth Symposium on Rock Mechanics*, Penn. State Univ., 12–14 June, Am. Soc. Civ. Eng. 649–687 (1973).
28. Turner F. J., Griggs D. T. & Heard H. Experimental deformation of calcite crystals. *Bull. geol. Soc. Am.* **65**, 883–934 (1954).
29. Wawersik W. R. & Brace W. F. Post-failure behavior of a granite and diabase. *Rock Mech.* **3**, 61–83 (1971).
30. Zener C. The micro-mechanism of fracture. *in Fracturing of Metals* (Edited by Jonassen F., Roop W. P. & Bayless R. T.) Am. Soc. Met., Cleveland (1948).